Int. J. Electrochem. Sci., 12 **(2017)** 5284 – 5293, doi: 10.20964/2017.06.54

International Journal of
ELECTROCHEMICAL
SCIENCE
www.electrochemsci.org

Short Communication

Hydrogen Peroxide Activated Commercial P25 TiO_2 as Efficient Visible-light-driven Photocatalyst on Dye Degradation

Shifei Kang[*], *Lu Zhang, Chenglu Liu, Lihua Huang, Huancong Shi, Lifeng Cui*[*]

Department of Environmental Science and Engineering, University of Shanghai for Science and Technology, Shanghai, 200093, China.
[*]E-mail: sfkang@usst.edu.cn, lifeng.cui@gmail.com,

Received: 1 March 2017 / *Accepted:* 19 April 2017 / *Published:* 12 May 2017

The extension of the photoactive wavelength region of TiO_2 photocatalysts into the visible region is desirable for popularizing TiO_2 photocatalysts into practice. Among all the strategies to modifying TiO_2, the presence of hydrogen peroxide (H_2O_2) was report to be able to induce visible-light activity for bare TiO_2. However, the activation mechanism of this cheap and convenient proposal for the photocatalytic activity improving of TiO_2 was still not completely understood. In this work, commercial available P25 TiO_2 was used to verify the sensitization effect of H_2O_2 surface modification. Remarkably, the RhB photocatalytic degradation over P25 TiO_2+H_2O_2 sample is efficient and nearly 60% of the dye is completely removed after 210 min under visible light irradiation, which indicates the excellent photocatalytic performance of hydrogen peroxide treated P25 TiO_2. Electrochemical impedance spectroscopy (EIS) was employed to determine the electrical conductivity and photogenerated charge separation character of P25 TiO_2 with or without H_2O_2 surface modification. Our results clearly support the commercial application of H_2O_2 activated P25 TiO_2 as efficient visible-light-driven photocatalyst.

Keywords: TiO_2, H_2O_2, Visible-light-driven Photocatalyst, Surface modification, Electrochemical impedance spectroscopy

1. INTRODUCTION

Nowadays, semiconductor based photocatalysis techniques are essential for both fundamental and practical perspectives, especially on dye staffs remove [1]. The dye staffs are commonly used in printing, pharmaceutical and leather industries. Most of dyes are recalcitrant molecules and recognized to be of synthetic origin and toxicity. The complex composition, chemical stability and high chemical oxygen consumption make these dyes refractory. Therefore, dye removal becomes a very important

but challenging area of wastewater treatment. Among all the semiconductor materials, the nanosized TiO_2 particles are used widely as one of the photocatalysts due to their low-cost, non-toxicity, chemical stability and high activity [2]. However, its high activity can be acquired only under ultraviolet light with a wavelength of 400nm or less, which is only 3-5% part [3, 4] of the solar spectrum, can be absorbed by TiO2 due to its wide intrinsic band gap. These seriously limit its application and development. Therefore, extension of the photoactive wavelength region of TiO_2 into the visible region is desirable for popularizing TiO_2 photocatalysts toward commercial applications [5], especially under solar light for industrial areas or poor interior lighting illumination in living spaces.

Over the past decade, strategies such as dye-sensitizing, non-metal doping, metal doping and semiconductor heterojunction construction have been comprehensively studied [6]. Recently, it was reported that the presence of hydrogen peroxide (H_2O_2) could be able to induce visible-light activity for bare TiO_2, which has little efficiency under visible-light itself. The mechanism of the visible-light activity of hydrogen peroxide treated TiO_2 was interesting and have attracted wide attention. Kim et al. [7] reported 4-chlorophenolandphenolic compounds in aqueous suspension of pure titania could be degraded under visible illumination. Nevertheless, the photocatalytic degradation reaction could only be triggered in the presence of electron acceptors, and hydrogen peroxide was accordingly considered as an electron acceptor in photocatalytic degradation reaction. Meanwhile, the TiO_2 samples changed to a yellow color when treated with peroxide hydrogen. Neither hydrogen peroxide nor titania alone can absorb visible light, but the -OOH groups of H_2O_2 replace -OH groups on the surface of titania forming yellow surface complexes due to the presence of H_2O_2 [8], which shift light absorption region of TiO_2 to visible light region. The coloration of TiO_2 particles by hydrogen peroxide is thought to be related to their photocatalytic activity under visible light. Rao and Chu [9] found that more than 70% linuron (LNR) could be decomposed by the TiO_2/H_2O_2 system under visible light irradiation. Wang and coworkers [10] treated nanotubular titanic acid with an aqueous solution of H_2O_2 to extend its light absorbance responses into the visible light region in order to enhance the photocatalytic activity for the oxidation of propylene under visible light irradiation [11]. The presence of H_2O_2 caused a red shift in the diffuse reflectance absorption spectra for a TiO_2 powder compared with the absence of H_2O_2, and there exists a tailing absorbance in the 400-500nm visible region.

Taking into account that H_2O_2 can serve as a reservoir of more active ROS and that the impact of these relatively stable ROS on the mechanism of photocatalysis is not clear, in this work we propose to investigate the impact of the H_2O_2 treatment on the physicochemical nature and visible-light photocatalytic activity of TiO_2. Meanwhile, considering that there are few reports focus on the sensitization of commercial available P25 TiO_2, which actually processed the most promising application potential among all the commercial TiO_2 materials, Herein we use P25 TiO_2 as the precursor to explore the commercial potential of hydrogen peroxide sensitization proposal on TiO_2 photocatalyst. Moreover, their photocatalytic capacities were investigated for the decolorization of synthetic wastewater containing Rhodamine B (RhB) which is a widely-used dye.

2. EXPERIMENTAL SECTION

2.1. Materials preparation

Rhodamine B (RhB) and hydrogen peroxide (H_2O_2, 30 wt.% in water) was obtained from Sinopharm group chemical reagent Co., Ltd. (China). The commercial titanium dioxide powder (P25 TiO_2) was obtained from Degussa CO., LTD. (Germany). All other reagents were analytical grade and used without further purification.

The hydrogen peroxide sensitized TiO_2 (P25 TiO_2+H_2O_2) photocatalyst was obtained by simple soak P25 TiO_2 in 3 wt.% H_2O_2 water solution with stirring for 1h then dried at 60 ^oC. To eliminate the influence of simple water wetting, The P25 TiO_2+H_2O sample as a referenced material was obtained by soak P25 TiO_2 in deionized water with stirring for 1h then dried at 60 ^oC.

2.2. Characterization

The phases of the products were characterized through X-ray diffraction method using CuK radiation (λ= 0.15418 nm) in a XD-3 diffractometer (Beijing Pgeneral). Fourier transform infrared (FT-IR) spectra in the region of 400-4000 cm^{-1} were recorded at room temperature with a Bruker IS-88 spectrometer (resolution 4 cm−1; 16 scans/spectrum). Catalyst powders were dispersed in KBr (0.6wt.% for all samples). The UV-vis spectra of the power photocatalysts were recorded on a spectrophotometer with an integrating sphere (Shmadzu UV-2550); $BaSO_4$ was used as a reference sample. For UV irradiation, a 400W UV lamp was used. For visible light irradiation, a 300W xenon lamp (HSX-F300, Beijing NBet) with a filter (λ> 420 nm) was used. Transmission electron microscopy (TEM) images were obtained with JEM-2100F microscope with an accelerating voltage of 200 kV. The electrochemical Impedance Spectroscopy **(**EIS) data were performed on an electrochemical workstation (CHI 660E, Shanghai Chenhua Instrument Company, China) based on a conventional three-electrode system with a frequency range from 0.01 Hz to 100 kHz at the circuit potential.

2.3. Photocatalytic degradation of RhB

RhB (10 mg/L) was selected as probe dyes to evaluate the photocatalytic activities of as-prepared photocatalysts. A 300W xenon lamp (HSX-F300, Beijing NBet) with a 420 nm cutoff filter was used as a visible light source to trigger the photocatalytic reaction. Prior to irradiation, the mixture was magnetically stirred for 30min to establish the adsorption/desorption equilibrium. In a typical run, 50mg photocatalyst power was added into 50 mL of RhB solution with a desired concentration. After a given irradiation time, 3mL of the mixture were sampled and withdrawn immediately after separating catalyst particles by centrifugation at 10000 r min^{-1}. The absorption spectrum of RhB solution was measured on a Shimadzu UV-2450 spectrophotometer.

3. RESULTS AND DISCUSSION

3.1. Crystal structure

Fig. 1 shows the X-ray powder diffraction (XRD) patterns of the bare P25 TiO_2, P25 TiO_2+H_2O and P25 TiO_2+H_2O_2 samples. From the XRD patterns, the peaks at 2θ = 25.3, 37.8, 48.0, 53.9, 55.1, 62.7, 68.9, 70.3 and 75.1^o can be indexed to crystal planes of anatase TiO_2 [12], while the planes at 2θ of ca. 27.4, 36.1 and 41.2º can be ascribed to rutile TiO_2 [13]. The major diffraction peaks of all samples are identical and appear at 2θ values of 25.3◦, assigned to the (101) diffraction planes of anatase TiO_2. These results clearly indicating that all the samples were composed of a mixture of anatase and rutile TiO_2, and the structures of P25 TiO_2 have not been affected by the integration with H_2O_2.

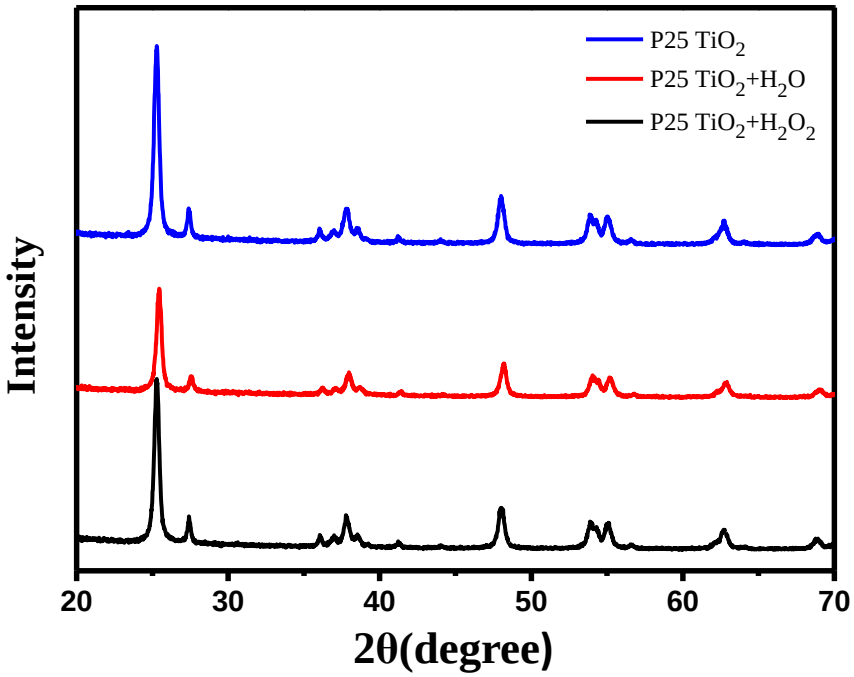

Figure 1. XRD patterns of the as-prepared samples

3.2. UV–vis spectra

Fig. 2 shows the UV-vis absorption spectra of the as-prepared samples. According to the picture, no absorption in the visible region (wavelength > 420nm) was observed but the strong absorption in the ultraviolet range for bare P25 TiO_2 and P25+H_2O, which meant the direct photocatalysis could not happen for P25 TiO_2 without treatment with H_2O_2 under visible light irradiation. The optical absorption edge was estimated at 426 nm for the P25 TiO_2+H_2O_2, 395nm for the P25 TiO_2+H_2O and 394 nm for the bare P25 TiO_2, and the corresponding band-gap energy was identified as 2.91 eV, 3.14 eV and 3.15 eV, respectively. The optical absorption edge appeared an obvious blue shift for the above samples relative to 425nm (about 2.91 eV) of the block anatase TiO_2.

And the original color of the P25 TiO_2 and P25 TiO_2+H_2O was white because the materials strongly absorbs wavelengths less than 394 nm, however, according to the formation of colored surface complexes, the color of the P25 TiO_2+H_2O changed to yellow correspondingly. Owing to their high dispersion and small size, the quantum size effect of nanosized nanoparticles could be evidence for this result [14].

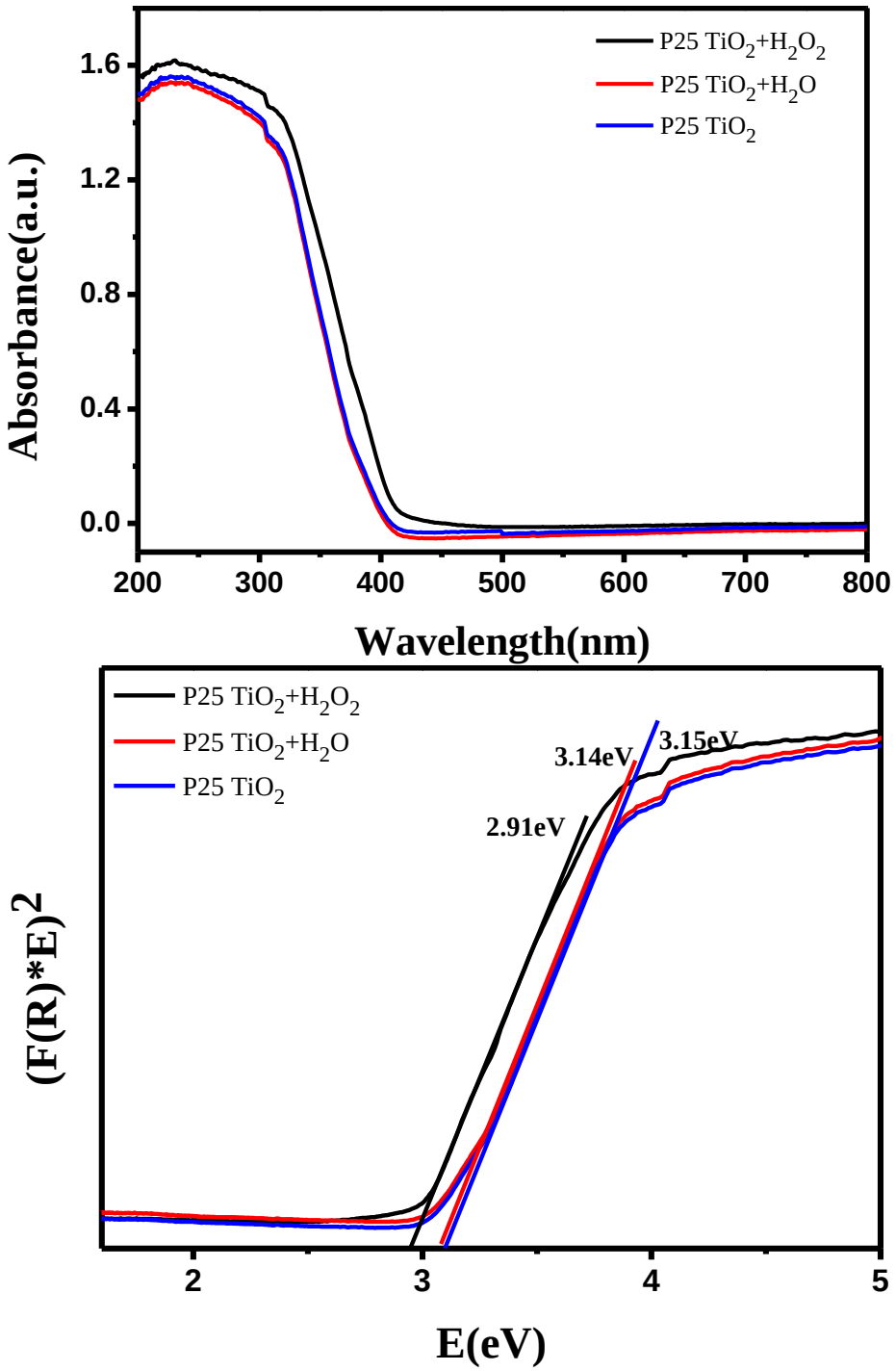

Figure 2. UV-vis spectra of the as-prepared samples

3.3.The FT-IR spectra

The FT-IR spectra obtained for all the catalysts showed some vibrations at 3300 cm^{-1} and between 1200 and 1800 cm^{-1}, which correspond to the vibration of the -OH groups and H_2O molecules [15, 16] adsorbed on the TiO_2 surface. Obviously, compared with bare Degussa P25 TiO_2, the P25 TiO_2+H_2O_2 sample processed enhanced absorption peak of surface adsorbed H_2O molecules, indicating that H_2O_2 treatment would increase the physisorbed water on TiO_2, which is beneficial in formation of hydroxyl radicals and promoting the photoactivity [17] of the P25 TiO_2 photocatalyst.

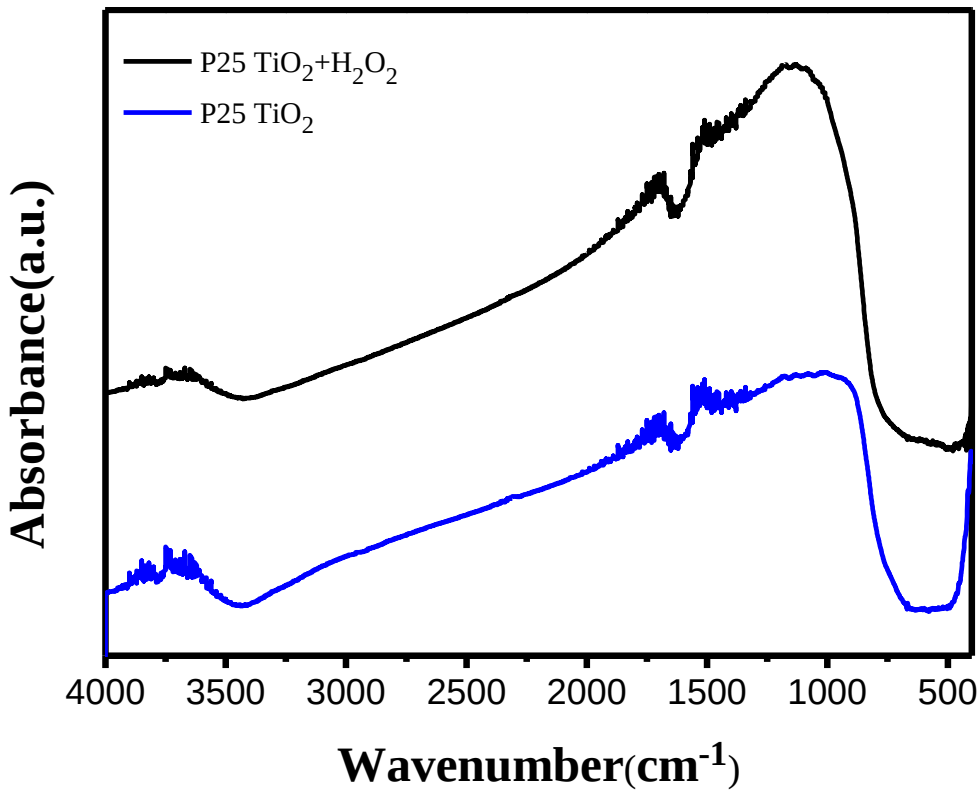

Figure 3. The FT-IR spectra of the as-prepared samples

3.4. Morphology

The TEM images of P25 TiO_2; (b) and (d) P25 TiO_2+H_2O_2 was shown in Fig.4.The pure TiO_2 nanocrystals were highly crystallized, as seen from the well resolved lattice features shown in the highresolution TEM (HRTEM) image (Fig.4a and c); the size of individual TiO_2 nanocrystals was approximately 10-20 nm in diameter. After hydrogenation, however, the surfaces of TiO_2 nanocrystals became disordered (Fig.4b and d) where the disordered outer layer surrounding a crystalline core was 1nm in thickness. This disorder layer serves in facilitating the charge separation in photocatalytic process.

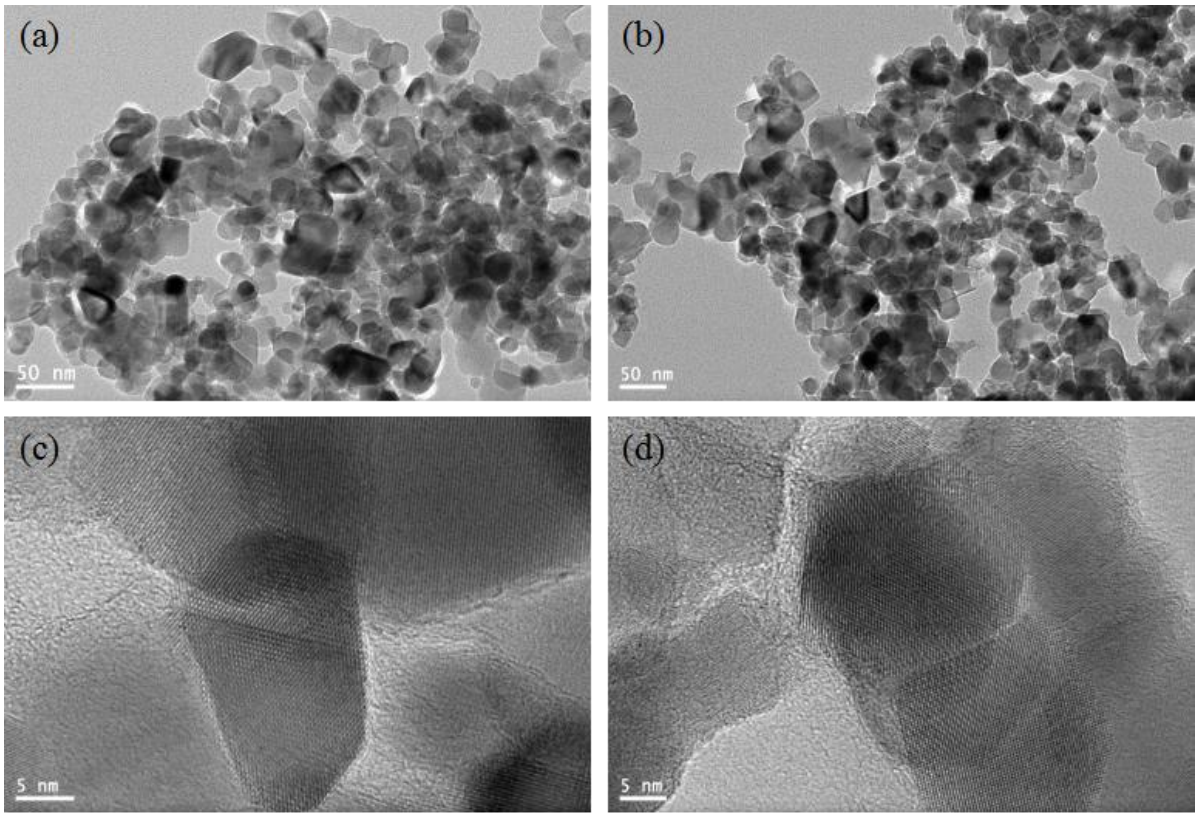

Figure 4. TEM images of the as-prepared samples: (a) and (c) P25 TiO_2; (b) and (d) P25 TiO_2+H_2O_2.

3.5. Photocatalytic activity

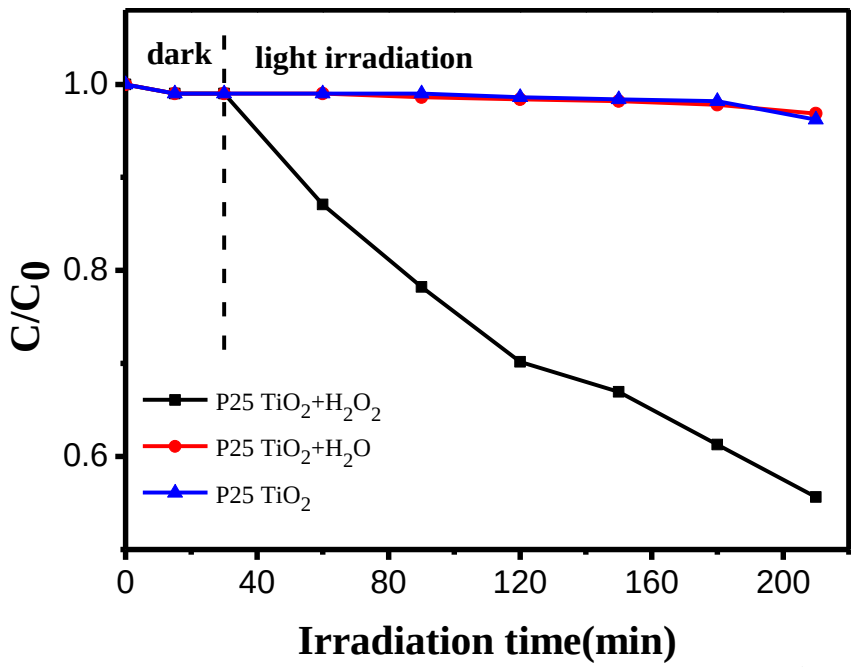

Figure 5. Photodecomposition curves of RhB dye in solutions (10 mg·L^{-1}) under visible light irradiation over different photocatalysts. *C* is the concentration of RhB dye at time t, and C_0 is that in the RhB solution immediately after it is kept in the dark to reach the equilibrium adsorption state.

Some researches have demonstrated that the titanium peroxide complex could account for the visible-light activity of the P25 TiO_2 photocatalyst, whereas the residual H_2O_2 in the solution may function as an external electron acceptor to reduce the recombination of charge carriers. Herein, the role of residual H_2O_2 in the solution was investigated using two treatments (with H_2O_2 and H_2O) under visible light ($\lambda > 420$ nm). Figure 4 shows the RhB photodegradation efficiency as a function of irradiation time under visible light irradiation, where C_0 and C are the RhB concentrations after adsorption-desorption equilibration and after certain period of irradiation, respectively. No obvious photodegradation are detected in the contrast experiments using P25 TiO_2+H_2O and pure P25 TiO_2 under visible light, which verified the high structural stability of RhB in this test condition. Remarkably, the RhB photocatalytic degradation over P25 TiO_2+H_2O_2 sample is efficient and nearly 60% of the dye is completely removed after 210 min of irradiation, which indicate the excellent visible-light-driven photocatalytic performance of P25 TiO_2+H_2O_2.

3.6. Electrochemical impedance spectroscopy

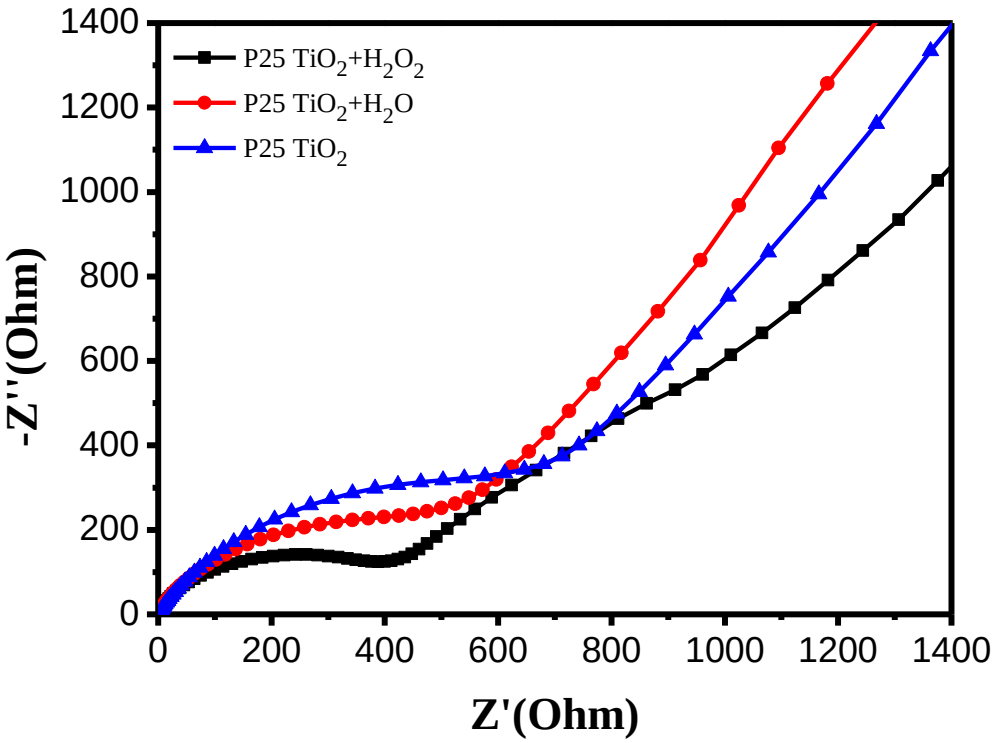

Figure 6. Plots of photogenerated carriers trapped during the photocatalytic degradation of RhB.

To investigate the mechanism of P25 TiO_2 sensitization by H_2O_2, the electrical conductivity and photogenerated charge separation character were determined via electrochemical impedance spectroscopy (EIS). The EIS Nyquist plots of P25 TiO_2+H_2O_2, P25 TiO_2+H_2O and the Degussa P25 TiO_2 electrodes under visible light irradiation are shown in Fig.5. The arc radius on EIS Nyquist plot of P25 TiO_2+H_2O_2 is smaller than other samples. As reported, a smaller arc radius of the EIS Nyquist plot suggests a more effective separation of photogenerated electron-hole pairs and the faster interfacial

charge transfer [18, 19]. These results suggest the P25 TiO_2+H_2O_2 sample has dramatically smaller charge transfer resistance and higher electron-hole separation/transfer efficiency. The enhanced photoelectric properties can be attributed to the surface disorder layer that greatly facilitates the mass transfer and improves photogenerated charge mobility [8].

3.7. Mechanism of sensitization

Even the research on the sensitization of commercial available P25 TiO_2 by hydrogen peroxide was rare, there are already reports focus on the sensitization mechanism of H_2O_2 on other types TiO_2. The research team of Li [8] reported the following conceptual mechanism: the surface of TiO_2 would be modified with -OOH groups through adsorbed H_2O_2 molecules to form the surface titanium-(Ⅳ) hydrogen peroxide complexes(>Ti-OOH) which could generate titania with excess interstitial oxygen defects. Those defects interact with lattice oxygen atoms, resulting in an increase in the lattice parameters and therefore a decrease in the band gap, and thus enhance the visible-light photoresponse.

For the current used P25 TiO_2+H_2O sample, as discussed above, more physisorbed water molecules would make against the direct interaction of H_2O_2 to TiO_2, leading to less capture of electron accordingly. As a result, for the P25 TiO_2+H_2O sample, the separate effect of electron and hole pairs could be ignored as indicated in the result of EIS in Fig.6. In our study, the positive effect of H_2O_2 could be ascribed to its dependence on the surface chemistry of TiO_2 particles. Because for the P25 TiO_2+H_2O_2 sample, the excited electrons would be recombined in the impurity states without H_2O_2, resulting in low activity. However, the addition of H_2O_2 can remarkably restrain the recombination of charge carriers [20-22]. In addition, the valuable hydroxyl radicals (HO•) would be scavenged by the excess H_2O_2 molecules to form much weaker oxidant HO_2• [23-25]. Therefore, the balance of two photochemistry action of H_2O_2 for TiO_2 sol systems would result in the increase of hydroxyl radicals.

4. CONCLUSIONS

After sensitized with H_2O_2, there exists the peroxide complexes on TiO_2 surface, so that the P25 TiO_2 could absorb visible light. The P25 TiO_2 treated with H_2O_2 exhibited the inferior visible light absorption and photoactivity under visible light irradiation. As a consequence of the formation of more peroxide complexes and hydroxyl radicals, TiO_2 with the H_2O_2 treatment would increase the physisorbed water on it, which thus increased photoactivity of the photocatalyst. The photocatalytic degradation rate of RhB dye over P25 TiO_2+H_2O_2 sample is nearly 60% after 210 min under visible light irradiation, which imply the excellent potential of H_2O_2 sensitized P25 TiO_2 in photocatalytic applications. Herein, the results presented here demonstrated that the sensitization of H_2O_2 could efficiently enhance photocatalytic performance of the commercial available P25 TiO_2 and realize the photocatalytic activity under visible light irradiation as expected.

ACKNOWLEDGEMENTS
This work was supported by National Natural Science Foundation of China (Grant No. 51528202 51671136 and 51502172), "Shu Guang" project (Grant No. 13SG46) supported by Shanghai Municipal Education Commission and Shanghai Education Development Foundation and Capacity-Building of Local University Project by Science and Technology Commission of Shanghai Municipality (Grant No. 12160502400).

References

1. S.F. Kang, Y. Fang, Y.K. Huang, L.F. Cui, Y.Z. Wang, H.F. Qin, Y.M. Zhang, X. Li, Y.G. Wang, *Appl. Catal. B-Environ.*, 168, (2015), 472-482.
2. M. Bellardita, A. Di Paola, B. Megna, L. Palmisano, *Appl. Catal. B-Environ.*, 201, (2017), 150-158.
3. J. Podporska-Carroll, A. Myles, B. Quay, D.E. McCormack, R. Fagan, S.J. Hinder, D.D. Dionysiou, S.C. Pillai, *J. Hazard. Mater.*, 324, (2017), 39-47.
4. H.X. Li, Z.F. Bian, J. Zhu, Y.N. Huo, H. Li, Y.F. Lu, *J. Am. Chem. Soc.*, 129, (2007), 4538-+.
5. J.Y. Lee, W.K. Jo, *Ultrason. Sonochem.*, 35, (2017), 440-448.
6. Y.G. Wang, Y.T. Chen, Y.H. Zuo, F. Wang, J. Yao, B. Li, S.F. Kang, X. Li, L.F. Cui, *Catal. Sci. Technol.*, 3, (2013), 3286-3291.
7. S. Kim, W. Choi, *J. Phys. Chem. B.*, 109, (2005), 5143-5149.
8. X.Z. Li, C.C. Chen, J.C. Zhao, *Langmuir.*, 17, (2001), 4118-4122.
9. Y.F. Rao, W. Chu, *Environ. Sci. Technol.*, 43, (2009), 6183-6189.
10. Y. Wang, X.J. Meng, X.L. Yu, M. Zhang, J.J. Yang, *Appl. Catal. B-Environ.*, 138, (2013), 326-332.
11. Y. Li, C.Y. Yang, S.M. Chen, *Int. J. Electrochem. Sc.*, 6, (2011), 4829-4842.
12. C.M. Yang, P.W. Chen, C.J. Liu, S.Y. Chen, C.S. Kuo, I.G. Chen, M.K. Wu, *Ieee. T. Appl. Supercon.*, 27, (2017).
13. H. Xu, Q. Zhang, W. Yan, W. Chu, L.F. Zhang, *Int. J. Electrochem. Sc.*, 8, (2013), 5382-5395.
14. J. Zhang, Z.W. Wang, Q.Y. Wang, C. Pan, Z.C. Wu, *J. Membrane. Sci.*, 525, (2017), 378-386.
15. L.L. Yang, X.Y. Ma, W.H. Zhang, W. Gen, *J. Appl. Polym. Sci.*, 134, (2017).
16. I. Ali, S.R. Kim, S.P. Kim, J.O. Kim, *Catal. Today.*, 282, (2017), 31-37.
17. C.S. Guo, K. Wang, S. Hou, L. Wan, J.P. Lv, Y. Zhang, X.D. Qu, S.Y. Chen, J. Xu, *J. Hazard. Mater.*, 323, (2017), 710-718.
18. X.J. She, H. Xu, Y.G. Xu, J. Yan, J.X. Xia, L. Xu, Y.H. Song, Y. Jiang, Q. Zhang, H.M. Li, *J. Mater. Chem. A.*, 2, (2014), 2563-2570.
19. H. Xu, J. Yan, X.J. She, L. Xu, J.X. Xia, Y.G. Xu, Y.H. Song, L.Y. Huang, H.M. Li, *Nanoscale.*, *6*, (2014), 1406-1415.
20. C.C. Chen, X.Z. Li, W.H. Ma, J.C. Zhao, H. Hidaka, N. Serpone, *J. Phys. Chem. B.*, 106, (2002), 318-324.
21. W. Zhao, C.C. Chen, X.Z. Li, J.C. Zhao, H. Hidaka, N. Serpone, *J. Phys. Chem. B.*, 106, (2002), 5022-5028.
22. H.Y. Zhao, Y. Chen, Q.S. Peng, Q.N. Wang, G.H. Zhao, *Appl. Catal. B-Environ.*, 203, (2017), 127-137.
23. T.X. Liu, X.M. Li, X. Yuan, *J. Mol. Catal. A-Chem.*, 414, (2016), 122-129.
24. J. Zou, J.C. Gao, F.Y. Xie, *J. Alloy. Compd.*, 497, (2010), 420-427.
25. J. Zou, J.C. Gao, Y. Wang, *J. Photoch. Photobio. A.*, 202, (2009), 128-135.